

Performance estimation of Savonius wind and Savonius hydrokinetic turbines under identical power input

Cite as: J. Renewable Sustainable Energy **10**, 064704 (2018); <https://doi.org/10.1063/1.5054075>

Submitted: 29 August 2018 • Accepted: 05 November 2018 • Published Online: 28 November 2018

Parag K. Talukdar, Vinayak Kulkarni and Ujjwal K. Saha

COLLECTIONS

 This paper was selected as an Editor's Pick



[View Online](#)



[Export Citation](#)



[CrossMark](#)

ARTICLES YOU MAY BE INTERESTED IN

[Experimental studies of Savonius wind turbines with variations sizes and fin numbers towards performance](#)

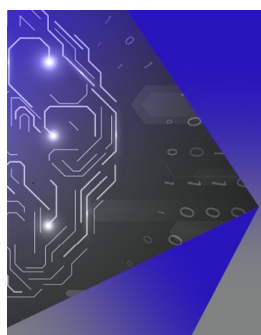
AIP Conference Proceedings **1931**, 030041 (2018); <https://doi.org/10.1063/1.5024100>

[Summary of Savonius wind turbine development and future applications for small-scale power generation](#)

Journal of Renewable and Sustainable Energy **4**, 042703 (2012); <https://doi.org/10.1063/1.4747822>

[Effect of blades number to performance of Savonius water turbine in water pipe](#)

AIP Conference Proceedings **1931**, 030046 (2018); <https://doi.org/10.1063/1.5024105>



APL Machine Learning

Machine Learning for Applied Physics
Applied Physics for Machine Learning

**First Articles
Now Online!**

Performance estimation of Savonius wind and Savonius hydrokinetic turbines under identical power input

Parag K. Talukdar, Vinayak Kulkarni,^{a)} and Ujjwal K. Saha

Department of Mechanical Engineering, Indian Institute of Technology Guwahati, Guwahati 781039, India

(Received 29 August 2018; accepted 5 November 2018; published online 28 November 2018)

In the context of energy crisis, extensive depletion of fossil fuel, and climate change, the vertical-axis Savonius-type wind or hydrokinetic turbines appear to be promising candidates to extract energy from wind or free-flowing water because of their superior self-starting capability and design simplicity. The present investigation focuses on comparative analysis between Savonius wind turbines (SWTs) and Savonius hydrokinetic turbines (SHTs) at the same input power. To accomplish this, two configurations are considered, viz., 2-bladed and 3-bladed turbine designs having semicircular blade profiles. Experimental studies revealed that the SWTs operate in a slightly wider range of tip-speed ratios than the SHTs. It is also observed that, like SHTs, 2-bladed SWTs result in an improved (47%) peak power coefficient ($C_{P\max}$) than 3-bladed SWTs. In line with this, the computational studies, conducted to complement the experimental analysis, showed the superiority of 2-bladed SWTs over the 3-bladed SWTs. Both experimental and computational analyses reveal that the SHTs and SWTs show identical drag and lift characteristics for given kinetic energy of the inlet fluid stream. *Published by AIP Publishing.* <https://doi.org/10.1063/1.5054075>

I. INTRODUCTION

Among the possible renewable energy sources, wind energy and hydrokinetic energy are the potential sources as they are abundant, efficient, sustainable, and environmentally friendly. On account of this, researchers across the globe have carried out investigations on a range of wind and hydrokinetic turbine designs.^{1–4} Ozgener⁵ demonstrated that installation of a wind turbine system of 1.5 kW capacity in Turkey is a viable option for small-scale power generation. The analysis reported by Mohammadi and Mostafaeipour⁶ indicated a 50 kW capacity wind turbine to be an economical solution for electricity generation in Iran.

Similar to wind power extraction systems, hydrokinetic technologies can also convert instream hydrokinetic power mainly from tidal currents, rivers, streams, and ocean currents into useful electricity. Upon installation, these technologies can significantly impact the power portfolios of remote locations which do not have access to electricity. In that context, the drag-based vertical-axis Savonius turbines can be used to extract wind and hydrokinetic energies for small-scale power generation.

The Savonius turbine was developed and patented by the Finnish engineer Savonius in 1925. Its design was based on the modification of the “S” rotor. Hence, its appearance resembles the letter “S” when viewed from the top (Fig. 1). This turbine design is composed of two semi-circular shaped blades/buckets placed in such a way that the concave part of one blade faces the other but with a slight overlap in the middle.⁷ This type of turbine produces mechanical power because of the difference in drag force acting on the concave and convex sides of the blades. The drag force induces rotation when subjected to wind/water flows.⁸ These turbines are usually coupled to a generator through a gearbox to produce electricity. Despite knowing that the Savonius turbines possess low efficiency, it is favored since it is simple in design and

^{a)}Author to whom correspondence should be addressed: vinayak@iitg.ac.in

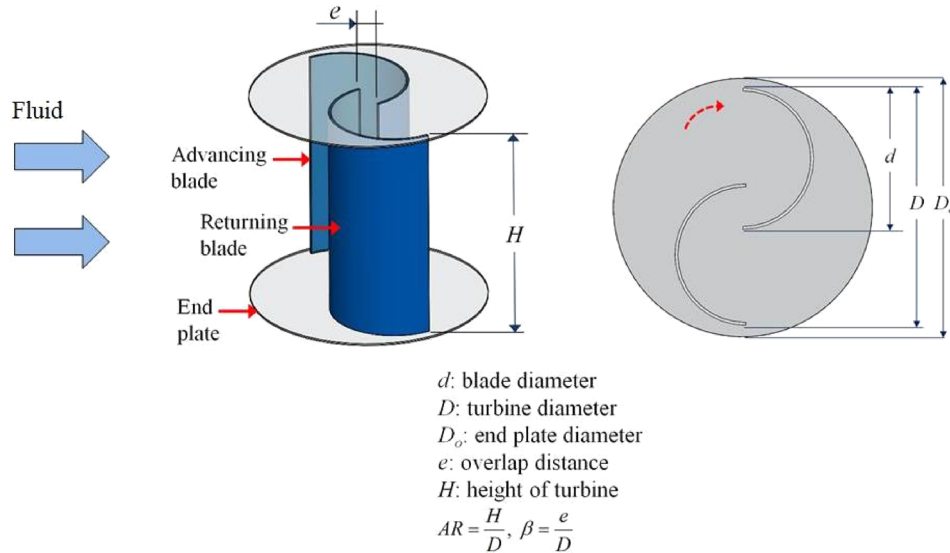


FIG. 1. Schematic of a vertical-axis Savonius turbine.

has lesser manufacturing cost than the lift-based Darrieus turbines. It has many advantages such as good starting characteristics, ease of installation and maintenance, absence of the yaw mechanism, low noise level, compact in size, and omnidirectional rotation.^{9–11} The low rotational speed is the prime reason for its reduced noise emissions and vibration.

Since its inception, a wide range of Savonius wind turbine (SWT) and Savonius hydrokinetic turbine (SHT) models were experimentally and numerically tested by the researchers for different design configurations and by employing different augmentation techniques to achieve the improved performance. Based on the initial experiments of SWTs with semicircular shaped blades, Savonius⁷ stated the maximum power coefficient (C_{Pmax}) of 0.31. The subsequent investigations conducted by Savonius revealed a higher C_{Pmax} of 0.37 for the same turbine. However, the successive studies on the Savonius turbine by the other researchers did not reveal the same value of C_{Pmax} . While working with SWTs, the researchers such as Sheldahl *et al.*,¹² Sivasagaram,¹³ Kahn,¹⁴ Fernando and Modi,¹⁵ and Ushiyama and Nagai¹⁶ reported C_{Pmax} in the range of 0.15–0.25. Kamoji *et al.*¹⁷ analyzed the performance of SWTs by varying the number of stages from 1 to 3. They reported that, for the same turbine of $AR = 1.0$, the single-stage turbine performed better than the two- and three-stage turbines in terms of power coefficient (C_P) and torque coefficient (C_Q). Furthermore, no difference in the performance between the two- and three-stage turbines has been observed. Kamoji *et al.*¹⁸ reported a C_{Pmax} of 0.17 for 2-semicircular-bladed SWTs ($AR = 1$ and $\beta = 0.15$) at a tip-speed ratio (TSR) of 0.78. Amiri *et al.*¹⁹ carried out the investigation on the performance of modified SWTs by varying the number of blades (3, 4, and 6). The wind tunnel experiments revealed the superior performance of 3-bladed SWTs with a C_{Pmax} of 0.21 at $TSR = 0.50$. Furthermore, in 1989, the influence of the drag and lift coefficients on the performance of SWTs was reported by Chauvin and Benghrib.²⁰ They experimentally evaluated C_D and C_L on the semicircular-bladed SWT from the pressure difference between the upper and lower surfaces of the turbine blade.

Similar studies on SHTs are also available in the literature. Khan *et al.*²¹ reported the C_{Pmax} values of 0.038, 0.049, and 0.04 for single, double, and triple stage semicircular-bladed SHTs, respectively. From the experimental study conducted by Nakajima *et al.*²² it was observed that the C_P value of SHTs can be enhanced by 10% with the use of double-stage configuration having a 90° phase difference between the blades. Sawada *et al.*²³ reported that at static conditions, the SHT ($\beta = 0.21$) produces positive torque at all azimuthal angles due to the contribution of lift force around $\theta = 240^\circ\text{--}330^\circ$ and the pressure recovery phenomenon around $\theta = 120^\circ\text{--}210^\circ$. Furthermore, at the rotating condition, a significant contribution of lift force to

the dynamic torque has been observed by the authors for $\theta = 240^\circ\text{--}330^\circ$. However, for the same rotating condition, the effect of pressure recovery in the overlapping region is reported to be negligible. Sarma *et al.*²⁴ experimentally compared the performance of SWTs and SHTs under similar input conditions and reported the C_{Pmax} for SHTs to be 61.32% higher than that for a conventional SWT.

A. Objectives

The literature review underlines the enormous capability of hydro energy and wind energy for small-scale power generation. The advantages of SWTs and SHTs provide the necessary impetus to deploy them in rural areas for developing small-scale stand-alone power stations that can further be utilized in household or agricultural applications. Furthermore, Savonius turbines being simple to design and fabricate have been preferred while developing a SWT or a SHT based power generation system. However, it is possible to use or adopt the same Savonius turbine design in both (SWT and SHT) the applications depending upon the seasonal needs. However, there is an enormous difference in dynamics of wind and water flows over the turbine. It is mainly due to the fact that wind flow is primarily governed by a pressure difference, whereas the gravity is predominantly responsible for water flow.²⁵ Nevertheless, the flow physics associated with them is different mainly due to density and viscosity differences and hence, the Reynolds number difference between the working mediums. Therefore, it is desirable to understand the effect of output power of a Savonius design, for a given inlet kinetic energy of the fluid stream, while working as SWTs and SHTs.

Separate studies on the effect of different design parameters on the performance of SWTs or SHTs are reported in the literature. However, a comprehensive analysis of a Savonius design for known input kinetic energy but with a difference in the working fluid medium is rarely reported. Therefore, in the present analysis, an attempt has been made to compare the performance of SWTs and SHTs having an identical kinetic energy of the oncoming fluid (wind/hydro). Further, studies are also extended to understand the performance alteration of the design with a change in the number of blades of the same shape with an imposed change in the medium of fixed kinetic energy. In order to achieve these objectives, initially, wind tunnel experiments with SWTs have been carried out and those are then compared with the equivalent SHT testing. Computational simulations are also performed to get better insights into the flow physics. Furthermore, the lift-drag characteristics of the SWTs and SHTs are discussed to support the experimental observations. Details of turbine designs, experimental setups, experimental results, and associated discussion are given in Secs. I B, II, and V A.

B. Turbine design

The major design parameters that generally affect the performance of the Savonius turbine are as follows: aspect ratio (AR), overlap ratio (β), number of blades (n), turbine stages, blade shape, shaft, and end plates.^{26,27} Thus, the components of the Savonius rotor include two end-plates, two or three blades, and one central shaft. It is reported that the overlap distance between the blades improves the C_P value of the turbine.²⁸ Furthermore, the addition of end plates helps in maintaining the pressure difference between concave and convex surfaces of the blades throughout the height of the turbine. Thus, the turbine having endplates is reported to yield higher C_P than that of the turbine without the endplates.^{26,27,29} Regarding the optimal size of the end plate diameter (D_o), there exists a consensus in the literature to make D_o to be equal to 1.1 times the turbine diameter (D).^{28,30,31}

In the present investigations, two turbine configurations listed in Table I have been considered, keeping the cross-sectional area (A) of the turbines fixed at 0.0625 m^2 ($D = 0.25 \text{ m}$ and $H = 0.25 \text{ m}$) while maintaining the overlap ratio ($\beta = 0.15$) and aspect ratio ($AR = 1$). Furthermore, the end plates having a diameter ($D_o = 1.1 \times D$) of 277.20 mm have been used to hold the blades in position. The chord length of the blade (d) is taken as 144 mm, and blades are fabricated from 1.3 mm thick mild steel sheets (Fig. 2).

TABLE I. Design specifications of turbines.

Design	No. of blades (n)	Blade shape	Overlap ratio (β)	Aspect ratio (AR)
I	2	Semicircular	0.15	1
II	3	Semicircular	0.15	1

C. Performance parameters

The performance of a Savonius turbine can be expressed in the form of power coefficient (C_P), torque coefficient (C_Q), and tip-speed ratio (TSR). These parameters are given by the following equations:^{31–34}

$$C_P = \frac{P_{\text{turbine}}}{P_{\text{kinetic}}} = \frac{T\Omega}{\frac{1}{2}\rho AV^3}, \quad (1)$$

$$T = 9.81 \times (W - S) \times r_p, \quad (2)$$

$$C_Q = \frac{2T}{\rho AV^2 R} = \frac{C_P}{TSR}, \quad (3)$$

$$TSR = \frac{\Omega R}{V}. \quad (4)$$

The fluctuation of torque is depicted by maximum and the minimum value of the torque measured in a complete revolution of the turbine. In general, this fluctuation is denoted by a non-dimensional parameter, ripple factor or rate of pulsation (γ), given in Eq. (5). Here, γ is defined as the ratio of the difference in the maximum and the minimum torque value to the average generated torque^{35,36}

$$\gamma = \frac{T_{\max} - T_{\min}}{T_a}. \quad (5)$$

II. EXPERIMENTAL METHODOLOGY

The SHTs are tested in an open channel flume at water treatment plant, IIT Guwahati, India.³⁷ They are mounted at the converging section of the flume [Fig. 3(a)] in order to test at high inlet velocity (0.80 m/s) and accordingly higher kinetic energy of water (15.9 W). The

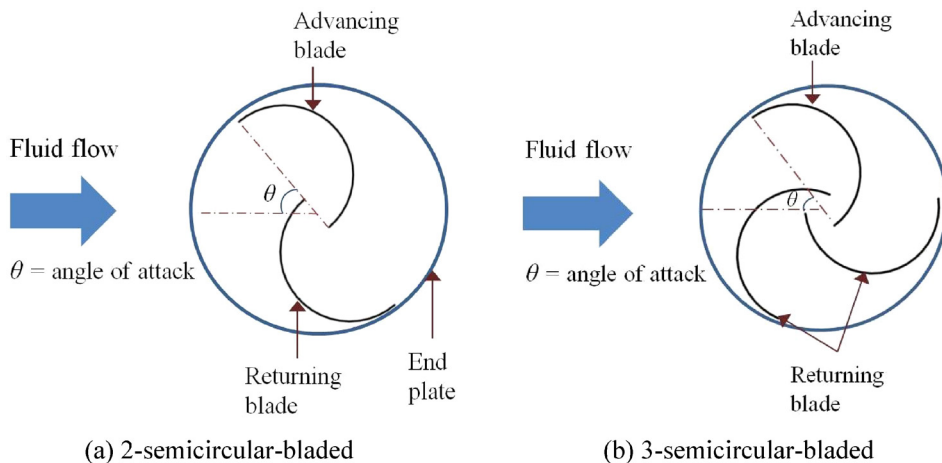


FIG. 2. Schematic diagram of the developed Savonius turbines.

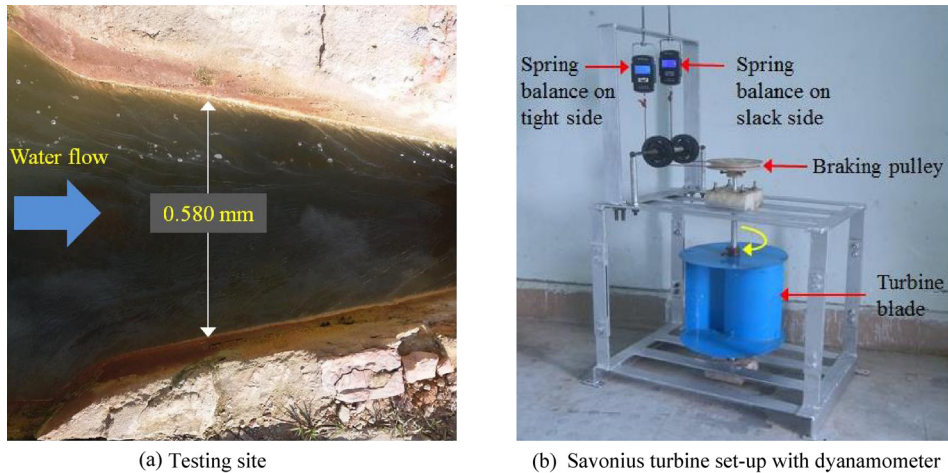
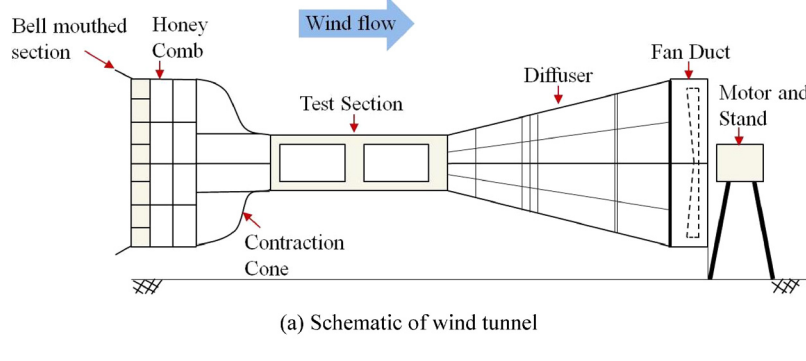


FIG. 3. Experimental facility for SHTs.

water depth available at the site was 0.40 m. The SHT test set-up with a mechanical dynamometer is shown in Fig. 3(b). Before actual experiments, the water velocity is measured at 3 different heights from the bottom surface of the channel, such as 20%, 60%, and 80% of total water depth for a given stream wise location. Thereafter, the arithmetic mean of all the readings was taken for further calculation.

By keeping an identical kinetic energy input to that of SHTs, the performances of the same turbine are evaluated, as a SWT, in a low-speed open circuit wind tunnel facility. This tunnel provides a uniform air velocity of known value in the test section. The facility is capable for testing various turbine models to obtain their performance characteristics. Figure 4(a) shows a



(a) Schematic of wind tunnel



(b) Mounted turbine set-up

FIG. 4. Wind tunnel test facility.

schematic diagram of the facility with different sections. The test section of size $2\text{ m} \times 0.6\text{ m} \times 0.6\text{ m}$ is equipped with four perspex windows for viewing inside the test section. Furthermore, a wooden window at the top is used for mounting of the turbine, and thus, the mounted turbine in the test section is shown in Fig. 4(b).

Here, the desired wind speed in the test section is obtained by adjusting the rotational speed of the fan. This fan is directly coupled to an AC motor whose speed can be varied using an AC motor controller. Then the air velocity at the inlet to the turbine is measured using an inclined manometer. In the present set-up a maximum air speed of 45 m/s can be achieved in the test section at about 1450 rpm of the tunnel fan.

In each case, the mechanical dynamometer is employed for the measurement of torque and eventually the power produced by the turbine. The methodology for the torque measurement followed is reported by the previous investigators.^{31,34,37,38} Such a dynamometer mainly consists of two spring balances (accuracy: $\pm 0.2\%$) and braking pulley mounted on the turbine shaft. The braking loads are gradually applied on the turbine shaft with the help of the load control mechanism. Several combinations of torque and tip-speed ratios (TSRs) are recorded during each experiment. For each applied load, the corresponding rotational speed is measured by using a contact-type tachometer (Model: Lutron DT-2235B, range: 0.5 – 19 999 RPM, accuracy: $\pm 0.15\%$).

III. COMPUTATIONAL METHODOLOGY

Two dimensional (2-D) computational fluid dynamics (CFD) simulations have been carried out to model the flow physics of SWT/SHT using ANSYS-Fluent by accounting the vertical symmetry of the turbine. The usefulness of such simulations is already reported in the literature.^{39–41} In the present study, the sliding mesh technique has been used as it is widely used by many researchers [Abraham *et al.*,⁴² Plourde *et al.*,⁴³ Kumar and Saini;⁴⁴ and Roy and Ducoin⁴⁶] to analyze the flow over SHT/SWT in order to capture the unsteady turbulent effects and to provide acceptable results.

A. Computational domain and meshing

For the present simulations, the overall computational domain is separated into two distinct regions: inner rotating region containing the turbine model and the surrounding static rectangular region as shown in Fig. 5. The diameter of the inner region is taken as thrice of the turbine diameter ($3D$), whereas the stationary rectangular domain has a width of $6D$ and a length of $10D$. The computational studies, with these dimensions of the domain, are performed without accounting the blockage ratios, 17% and 23%, associated with the testing of SWTs and SHTs, respectively. Refined meshing along with inflation layers is used near the turbine blades in order to capture the flow physics and resolve the boundary layer flow. Here, the first layer has a thickness of 0.01 mm, and the maximum number of layers is 15 with the growth rate of 1.2.

B. Details of the solver setup

The flow field around a Savonius turbine is complex in nature due to the flow separation, wake formation, and time dependent solution. Therefore, the flow is considered here as turbulent, and the turbulence flow model is incorporated for realistic modeling of wind/water flow. Furthermore, unsteady simulations have been carried out in order to model the accelerating flow at the tip of the blades and also to model the wake/vortices near the blades. A 2-D, incompressible, 2nd order implicit coupled flow solver of unsteady Reynolds-averaged Navier-Stokes (RANS) equations is chosen for the present simulations. The SIMPLE (Semi-Implicit Method for Pressure Linked Equations) algorithm with pressure–velocity coupling is incorporated to ensure a better stability of the solution.^{34,45,46} Furthermore, this algorithm has advantages of being computationally inexpensive, and it has faster convergence as compared to the other schemes. The non-dimensional wall distance ($y+$) is maintained to be less than 1. The shear stress transport (SST) $k-\omega$ turbulence model is utilized as it effectively captures near wall flow

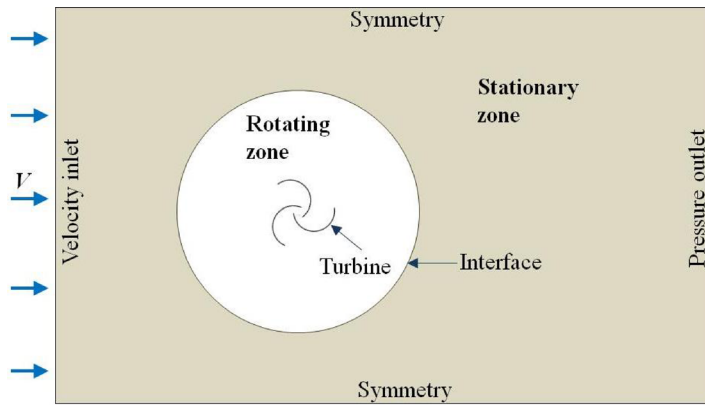


FIG. 5. Overall 2-D computational domain for 3-bladed turbines.

behavior and also for the free stream regions of the flow. This SST $k-\omega$ turbulence model has the features of both $k-\omega$ and $k-\epsilon$ turbulence models for near wall and far field calculations, respectively.^{46–48}

C. Boundary conditions

The boundary conditions imposed in the present study are shown in Fig. 5. In the case of SWTs, a uniform wind velocity (V) of 7.4 m/s is applied at the inlet, whereas for SHTs, $V=0.8$ m/s is set. Furthermore, no-slip boundary conditions are given at the turbine blades and the outlet is assigned as the pressure outlet (atmospheric pressure). The rotating zone is imposed to have certain rotational speed according to TSR through the sliding mesh interface, while the outer rectangular domain is maintained stationary (Fig. 6). The symmetry boundary conditions are given to the top and bottom extremities of the domain to ensure zero velocity normal to that boundary.^{34,37,41,46}

D. Grid independence test

The mesh density independence is evaluated for four refinement levels with the number of elements ranging from 26 183 to 122 944. It is observed that simulation with 94 216 and 122 944 results in the same value of C_P as shown in Fig. 7. Hence, the computational domain having a number of 94 216 elements has been opted for further studies as it would take lesser computational time than the simulation with further finer mesh but with the same accuracy.

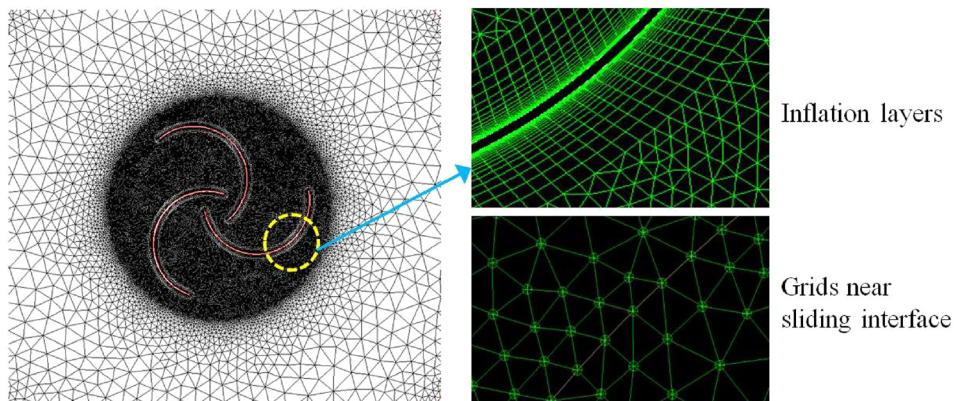
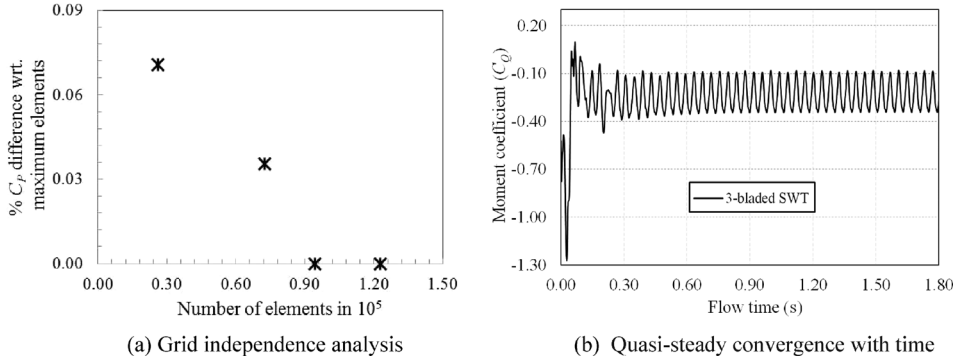


FIG. 6. Meshing near turbine blades and the interface.

FIG. 7. Grid independence and moment convergence for 3-bladed SWTs ($TSR = 0.72$).

IV. UNCERTAINTY ANALYSIS

The uncertainty calculation for the present experimental study has been carried out with established methods.^{49,50} The uncertainties of the tip-speed ratio (TSR) and power coefficient (C_P) are evaluated using Eqs. (6) and (7). In the case of SHTs, the uncertainties in the measurement of TSR and C_P are around $\pm 1.51\%$ and $\pm 2.13\%$, respectively. Similarly for SWTs, the uncertainties associated with TSR and C_P estimation are ± 2.01 and ± 2.98 , respectively

$$\frac{\partial(TSR)}{TSR} = \sqrt{\left(\frac{\partial N}{N}\right)^2 + \left(\frac{\partial V}{V}\right)^2}, \quad (6)$$

$$\frac{\partial(C_P)}{C_P} = \sqrt{\left(\frac{\partial(TSR)}{TSR}\right)^2 + \left(2\frac{\partial V}{V}\right)^2 + \left(\frac{\partial T}{T}\right)^2}. \quad (7)$$

V. RESULTS AND DISCUSSION

The performances of SWTs and SHTs are evaluated at the same input power condition (15.9 W). The experiments have been carried out at various mechanical loading conditions, and the results are discussed in terms of C_P with TSR and C_Q with TSR . Simultaneously, the observations obtained from the CFD study, for the experimental conditions, are also discussed in this section to gather the knowledge of lift and drag characteristics of the turbines.

A. Load characteristic experiments

Performance parameters of SWTs and SHTs are plotted in Figs. 8 and 9 for their two and three blade configurations. Here, it is evident that, for the same kinetic energy of fluid, both

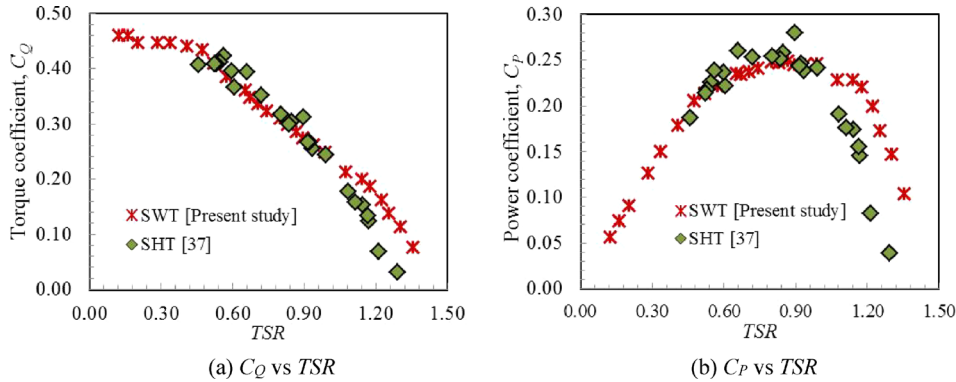


FIG. 8. Performance characteristics of 2-bladed turbines.

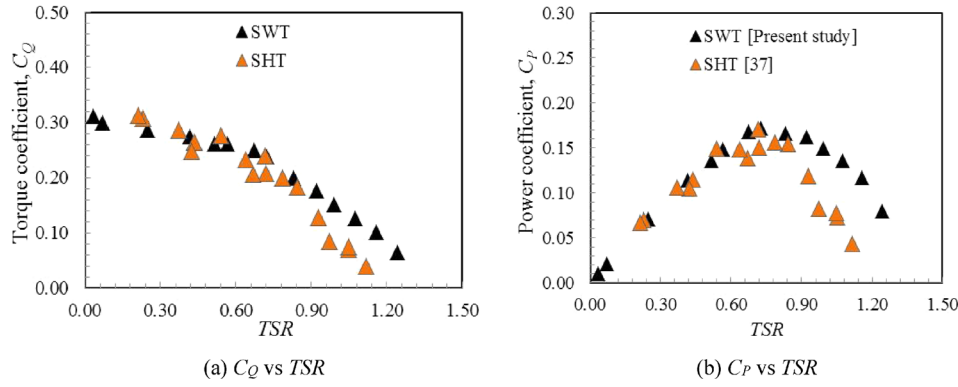


FIG. 9. Performance characteristics of 3-bladed turbines.

trends of C_P vs TSR and C_Q vs TSR curves are similar for all the SWTs and SHTs. It is also observed that the SWTs operate in a slightly wider range of $TSRs$ as compared to those of SHTs, particularly towards the increased value of TSR beyond the optimum as per the C_P vs TSR plot. The 2-bladed SWT demonstrates $C_{Pmax} = 0.25$ at $TSR = 0.87$, whereas for the SHT, $C_{Pmax} = 0.28$ is obtained at $TSR = 0.89$. Furthermore, both the 3-bladed SWT and SHT have shown the same C_{Pmax} of 0.17 at $TSRs$ of 0.72 and 0.71, respectively. Thus, the 2-bladed SWT is found to have better performance as compared to the 3-bladed SWT. Similar findings are already noticed for the SHTs as well.³⁷ The 2-bladed SWT and SHT operate at $TSRs$ of 1.44 and 1.34 for no-load conditions. At similar conditions, the 3-bladed SWT and SHT operate at $TSRs$ of 1.35 and 1.18, respectively. Again, the maximum braking loads lead to the braking torques of 0.13 Nm and 1.17 Nm for the 2-bladed SWT and SHT, respectively. Similarly, for the 3-bladed SWT and SHT, the maximum braking torques are 0.085 Nm and 0.91 Nm, respectively. Thus, the experimental study clearly shows that the semicircular design of the Savonius turbine of 2- or 3-blade configuration has the potential to produce the same shaft power for a given inlet kinetic energy of the fluid while functioning as a SHT or a SWT. Furthermore, the 2-bladed SWT is found to be more efficient than the 3-bladed one, as in the case of SHTs, in generating the shaft power from the same kinetic energy of the fluid. In Table II, a comparison of present experimental data with the previously reported data has been made. The existing reported works by Sheldahl *et al.*,¹² Kamoji *et al.*,¹⁸ Fujisawa and Gotoh,⁵¹ Sanusi *et al.*,⁵² and Ali⁵⁶ on the 2-semicircular-bladed SWT having $AR = 1$ indicated C_{Pmax} in the range of 0.17–0.24. However, the present 2-bladed SWT ($AR = 1$) shows a slightly higher C_{Pmax} of 0.25. In similar lines, Sheldahl *et al.*¹² reported a C_{Pmax} of 0.15 for the 3-semicircular-bladed SWT having $AR = 1$, whereas the present 3-bladed SWT ($AR = 1$) shows a C_{Pmax} of 0.17.

B. Computational analysis

In this section, performances of the SWTs and SHTs are discussed through computationally obtained lift-drag characteristics.

1. Validation studies

The validation study of the computational model is done with the experimental data of the 3-bladed SWT. As seen in Fig. 10, the computational results show a similar trend and very good agreement with the experimental results. At $TSR = 0.72$, the C_P obtained in the present CFD study is found to deviate by 6.2% from the experimental C_P . Furthermore, the difference in the C_P value between these two is 14.5% at $TSR = 1.16$. This validated methodology is employed to understand the lift and drag characteristics of SWTs and SHTs.

2. Moment and Lift-drag characteristics

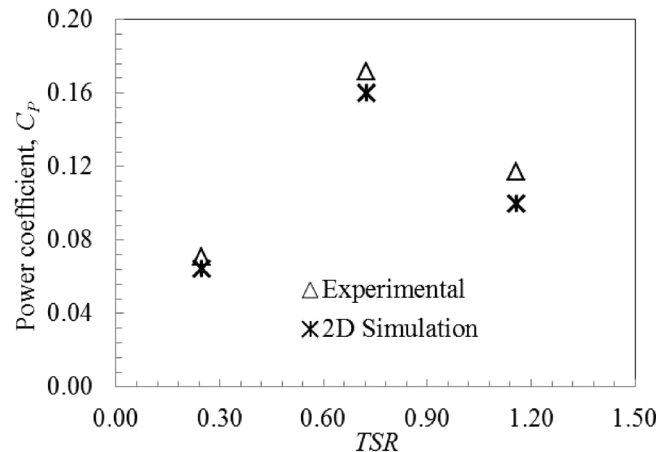
In Fig. 11, moment (torque) characteristics of the SWTs have been shown for one complete revolution of the turbines. The plot clearly shows higher magnitude of generated torque for the

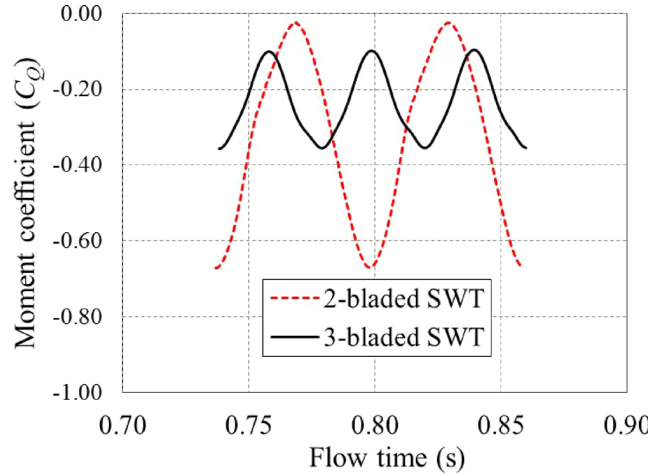
TABLE II. Summary of few reported studies on the Savonius turbine. CTS: Closed Test Section; OTS: Open Test Section.

Investigator(s)	Wind tunnel/field tests	Blade profile/working medium	C_{Pmax}	Optimum TSR
<i>2-bladed turbine</i>				
Sheldahl <i>et al.</i> ¹²	Wind Tunnel (CTS)	Semicircular (Wind)	0.24 ($AR = 1.0; \beta = 0.17$)	0.90
Kamoji <i>et al.</i> ¹⁸	Wind Tunnel (OTS)	Semicircular (Wind)	0.17 ($AR = 1.0; \beta = 0.15$)	0.78
		“Hook” shaped (Wind)	0.19 ($AR = 0.70; \beta = 0$)	0.72
Alom and Saha ³⁴	Wind Tunnel (OTS)	Elliptical (Wind)	0.14 ($AR = 0.70; \beta = e/d = 0.20$)	0.80
Fujisawa and Gotoh ⁵¹	Wind Tunnel (OTS)	Semicircular (Wind)	0.173 ($AR = 1.0; \beta = 0.15$)	0.90
Sanusi <i>et al.</i> ⁵²	Wind Tunnel (OTS)	Semicircular (Wind)	0.24 ($AR = 1.0; \beta = e/d = 0.15$)	0.78
Shankar ⁵³	Wind Tunnel (OTS)	Semicircular (Wind)	0.23 ($\beta = 0.05$)	0.85
Rabah and Osawa ⁵⁴	Field Tests	Semicircular (Wind)	0.24	0.60
Alexander and Holownia ⁵⁵	Wind Tunnel (CTS)	Semicircular (Wind)	0.14 ($AR = 1.25; \beta = 0.04$)	0.52
Ali ⁵⁶	Wind Tunnel (CTS)	Semicircular (Wind)	0.21 ($AR = 1; \beta = 0$)	0.80
Nakajima <i>et al.</i> ²²	...	Semicircular (Water)	0.25 ($AR = 1.48; \beta = 0.22$)	1.1
Patel <i>et al.</i> ²⁵	...	Semicircular (Water)	0.20 ($AR = 1.09; \beta = 0.13$)	0.55
Golecha <i>et al.</i> ⁵⁷	...	“Hook” shaped (Water)	0.14 ($AR = 0.7$)	0.70
Present study	Wind Tunnel (CTS)	Semicircular (Wind)	0.25 ($AR = 1.0; \beta = 0.15$)	0.87
<i>3-bladed turbine</i>				
Sheldahl <i>et al.</i> ¹²	Wind Tunnel (CTS)	Semicircular (Wind)	0.15 ($AR = 1.0; \beta = 0.17$)	0.70
Amiri <i>et al.</i> ¹⁹	Wind Tunnel (OTS)	Pivoted SWT (Wind)	0.21	0.50
Shankar ⁵³	Wind Tunnel (OTS)	Semicircular (Wind)	0.15 ($\beta = 0.05$)	0.85
Chen <i>et al.</i> ⁵⁸	Wind Tunnel (CTS)	Semicircular (Wind)	0.21 ($AR = 1.17; \beta = 0.17$)	0.64
Sarma <i>et al.</i> ²⁴	...	Semicircular (Water)	0.39 ($AR = 0.65; \beta = 0$)	0.77
Present study	Wind Tunnel (CTS)	Semicircular (Wind)	0.17 ($AR = 1.0; \beta = 0.15$)	0.71

2-bladed SWT, however with a higher ripple factor (γ). The γ values for 2-bladed and 3-bladed SWTs are obtained to be 1.88 and 1.25, respectively. Thus, the 3-bladed SWT offers smoother torque generation although it yields lesser torque output as compared the 2-bladed SWT. It is consistent with the experimental observation. In general, a minimum ripple factor is desirable for possible mechanical wear and longevity of the turbine.

The computationally obtained polar presentation of the lift coefficient (C_L) and drag coefficient (C_D) with respect to the angle of attack (θ) is presented in Fig. 12 to compare the

FIG. 10. Validation of CFD results with experimental data for 3-bladed SWTs ($TSR = 0.72$).

FIG. 11. Variations in C_Q for one revolution ($TSR = 0.87$).

performance of SWTs. The trend of the C_D curve for the 2-bladed SWT is found to be gradually increasing up to $\theta = 67^\circ$ and then gradually decreases up to $\theta = 162^\circ$ while following a similar pattern in the next cycle. However, in the case of the 3-bladed SWT, three peaks of C_D at 36° , 152° , and 273° can be observed because of the additional blade. The mean values of C_D are obtained as 1.22 and 1.17 for 2-bladed and 3-bladed SWTs, respectively, whereas the maximum C_D values for 2-bladed and 3-bladed SWTs are 1.81 and 1.45, respectively. In similar lines, the trend of the C_L curve for the 2-bladed SWT is found to be gradually increasing up to $\theta = 20^\circ$ and then gradually decreases up to $\theta = 120^\circ$ while following a similar pattern in the next cycle. For the 3-bladed SWT, the polar plot shows three peak values of C_L at 7° , 127° , and 247° . Similarly, the mean values of C_L are observed as 1.32 and 1.14 for 2-bladed and 3-bladed SWTs, respectively. Thus, it is quite evident that the 2-bladed SWT demonstrates better drag and lift characteristics, as compared to the 3-semicircular-bladed SWT like in the case of SHTs.³⁷ In both the 3-bladed SWT and SHT, excessive deflection of the working medium is expected as compared to that of a 2-bladed turbine. Such deflected stream otherwise would have struck on the following blade. The Coanda-type flow pattern at the down-stream of the advancing blade is destabilized due to the development of the large vortices in that region.³⁷ As a result of this, there is rise in the pressure downstream side of the advancing blade. Therefore, in the presence of the third blade, a lesser amount of available energy in the flowing

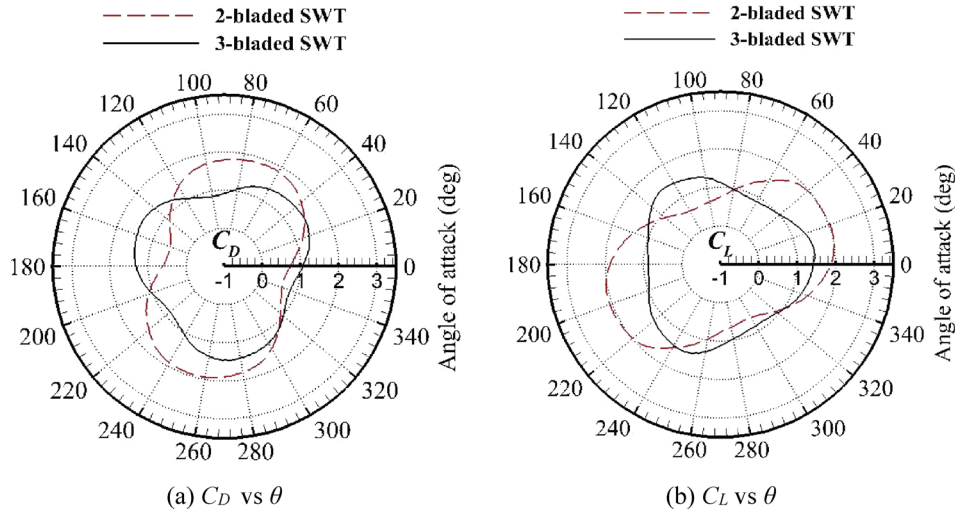


FIG. 12. Lift-drag characteristics of SWTs.

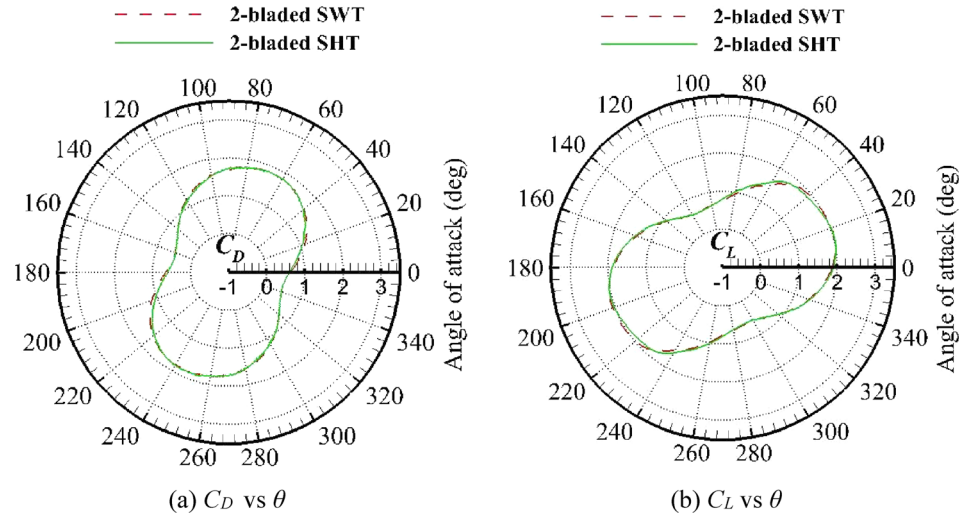


FIG. 13. Comparison of lift-drag characteristics for 2-bladed turbines.

water/wind gets converted into the mechanical energy by the turbine. Hence, there is reduction of maximum power and moment coefficients in a 3-bladed Savonius turbine as compared to the 2-bladed turbine. Previous experimental work reported by Irabu and Roy⁵⁹ indicated the maximum C_D for the 2-semicircular-bladed SWT to be 1.56 at $\theta = 90^\circ$ and 270° . Similarly, Jaohindy *et al.*⁶⁰ conducted numerical investigation to analyze the effect of C_D and C_L for a 2-semicircular-bladed SWT, and the maximum C_D is reported to be around 2.2 at an angle of attack (θ) in the range of 60° – 70° and at $TSR = 0.6$. Furthermore, at the same TSR , the value of maximum C_L is mentioned to be around 1.72 at $\theta = 30^\circ$ and 210° . Therefore, it is apparent that the present 2-bladed SWT is found to have demonstrated a nearly similar lift and drag characteristics in terms of C_D and C_L values. An equivalent observation has also been made about SHTs.³⁷

In similar lines, comparisons of lift-drag characteristics for SWTs and SHTs are presented in Figs. 13 and 14. It is evident that the SWT and SHT show almost the same lift-drag characteristics. Therefore, it can be concluded that irrespective of the fluid (wind/water) medium, the vertical-axis Savonius turbine generates approximately the same lift-drag characteristics for a given inlet power. Thus, the noticed similarity in the trend of load characteristic curves is consistent for 2- and 3-bladed SHTs and SWTs.

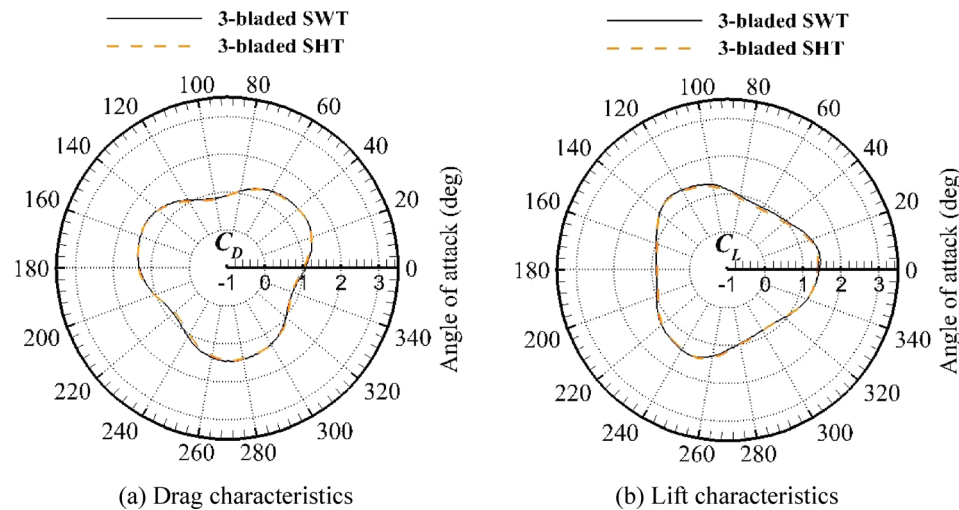


FIG. 14. Comparison of lift-drag characteristics for 3-bladed turbines.

VI. CONCLUSIONS

The vertical-axis Savonius turbine has the potential for small-scale electric power generation especially in rural areas. In this paper, a comparison of performance between the SHT and SWT has been done through experimental and 2-D CFD investigations. In that context, 2- and 3-bladed designs have been considered and tested under similar input power conditions of the fluids. The readings of SWTs and SHTs are obtained through wind tunnel and open channel testing for the identical input power condition of 15.9 W. The experimental readings are expressed here are in the form of power and torque coefficients as a function of the tip-speed ratio.

From the present investigation, the following conclusions may be drawn:

- The 3-bladed SWT has demonstrated the same value C_{Pmax} as that of the SHT, while the 2-bladed SHT shows almost similar performances as that of the SWT.
- The SWTs are found to operate in slightly wider ranges of TSR s than those of SHTs particularly towards the increased value of TSR beyond optimum TSR .
- The 3-bladed SWT demonstrates inferior performance than the 2-bladed SWT; however, it shows a smoother torque generation as compared to the later. The ripple factor for the 3-bladed SWT is obtained as 1.25, whereas for the 2-bladed SWT, it is observed to be 1.88.
- From the 2-D CFD analysis, the lift and drag characteristics of the SWTs have been analyzed. The improved performance of the 2-bladed SWT from the experimental study has been confirmed here. The variation of C_D with the angle of attack clearly indicates the higher magnitude of drag for the 2-bladed SWT over the 3-bladed SWT. Such observations are already made for SHTs.
- At identical input power, the SWTs and SHTs are found to demonstrate similar lift-drag characteristics which justify the fact that a turbine produces approximately the same power output for a given input power irrespective of the type of fluid.

The present research resulted in understanding the working of a Savonius turbine with a change in the fluid medium. The study highlights the superior performance of two-bladed turbines as compared to three-bladed turbines. In the present analysis, the Savonius turbines have been tested at only one particular input kinetic energy irrespective of the fluid. Thus, this study can be extended to analyze the turbine performances over a range of input kinetic energies along with a number of blade shapes. A detailed computational study can be pursued considering the effect of blockage for precise estimation of the turbine performances. Furthermore, the study on fatigue and stress analysis for SWTs and SHTs requires attention as force exerted by water on the turbine is significantly more than that by wind.

NOMENCLATURE

A	Swept area ($= D \times H$) [m^2]
CFD	Computational fluid dynamics
CTS	Closed test section
C_D	Drag coefficient
C_L	Lift coefficient
C_Q	Torque coefficient ($= \frac{T}{\frac{1}{2}\rho AV^2 R}$)
D	Diameter of the turbine [m]
D_o	Diameter of the end plate [m]
H	Height of the turbine [m]
k	Turbulence kinetic energy [m^2/s^2]
N	Rotational speed [rpm]
OTS	Open test section
$P_{kinetic}$	Kinetic power available in the fluid ($= \frac{1}{2}\rho AV^3$) [W]
$P_{turbine}$	Power output of the turbine ($= \frac{2\pi NT}{60}$) [W]
R	Radius of the turbine [m]
r_p	Radius of the pulley mounted on the central shaft [m]

S	Tension in the slack side [kg]
SHT	Savonius hydrokinetic turbine
SWT	Savonius wind turbine
T	Torque produced by the turbine ($= 9.81 \times (W - S) \times r_p$) [N m]
TSR	Tip-speed ratio ($= \frac{\omega R}{V}$)
T_a	Average generated torque [N m]
T_{max}	Maximum generated torque [N m]
T_{min}	Minimum generated torque [N m]
V	Free stream fluid velocity [m/s]
W	Tension in the tight side [kg]
y^+	Non-dimensional wall distance
β	Overlap ratio ($= \frac{e}{D}$)
γ	Ripple factor ($\gamma = \frac{T_{max} - T_{min}}{T_a}$)
ω	Specific rate of turbulent dissipation [1/s]
Ω	Angular speed [rad/s]
ρ	Density of fluid [kg/m ³]
θ	Angle of attack [°]

- ¹J. V. Akwa, H. A. Vielmo, and A. P. Petry, "A review on the performance of Savonius wind turbines," *Renewable Sustainable Energy Rev.* **16**, 3054–3064 (2012).
- ²H. M. S. M. Mazarbhuiya, A. Biswas, and K. K. Sharma, "Performance investigations of modified asymmetric blade H-Darrieus VAWT rotors," *J. Renewable Sustainable Energy* **10**, 033302 (2018).
- ³J. P. Abraham, B. D. Plourde, G. S. Mowry, W. J. Minkowycz, and E. M. Sparrow, "Summary of Savonius wind rotor development and future applications for smallscale power generation," *J. Renewable Sustainable Energy* **4**(4), 042703 (2012).
- ⁴P. K. Talukdar, V. Kulkarni, and U. K. Saha, "Field-testing of model helical-bladed hydrokinetic turbines for small-scale power generation," *Renewable Energy* **127**, 158–167 (2018).
- ⁵O. Ozgener, "A small wind turbine system (SWTS) application and its performance analysis," *Energy Convers. Manag.* **47**, 1326–1337 (2006).
- ⁶K. Mohammadi and A. Mostafaeipour, "Economic feasibility of developing wind turbines in Aligoodarz, Iran," *Energy Convers. Manag.* **76**, 645–653 (2013).
- ⁷S. J. Savonius, "The S-rotor and its applications," *Mech. Eng.* **53**(5), 333–338 (1931).
- ⁸I. Al-Bahadly, "Building a wind turbine for rural home," *Energy Sustainable Dev.* **13**, 159–165 (2009).
- ⁹J. L. Menet, "A double-step Savonius rotor for local production of electricity: A design study," *Renewable Energy* **29**, 1843–1862 (2004).
- ¹⁰U. K. Saha, S. Thotla, and D. Maity, "Optimum design configuration of Savonius rotor through wind tunnel experiments," *J. Wind Eng. Ind. Aerodyn.* **96**, 1359–1375 (2008).
- ¹¹M. A. Kamoji, S. B. S. Kedare, and V. Prabhu, "Performance tests on helical Savonius rotors," *Renewable Energy* **34**, 521–529 (2009).
- ¹²R. E. Sheldahl, B. F. Blackwell, and L. V. Feltz, "Wind tunnel performance data for two- and three-bucket Savonius rotors," *J. Energy* **2**(3), 160–164 (1978).
- ¹³S. Sivasesgaram, "Secondary parameters affecting the performance of resistance-type vertical-axis wind rotors," *Wind Eng.* **2**, 49–58 (1978).
- ¹⁴M. H. Kahn, "Model and prototype performance characteristics of Savonius rotor windmill," *Wind Eng.* **2**, 75–85 (1978).
- ¹⁵M. S. U. K. Fernando and V. J. Modi, "A numerical analysis of the unsteady flow past a Savonius wind turbine," *J. Wind Eng. Ind. Aerodyn.* **32**, 303–327 (1989).
- ¹⁶I. Ushiyama and H. Nagai, "Optimum design configurations and performance of Savonius rotors," *Wind Eng.* **12**, 59–75 (1988).
- ¹⁷M. A. Kamoji, S. B. Kedare, and S. V. Prabhu, "Experimental investigations on single stage, two stage and three stage conventional Savonius rotor," *Int. J. Energy Res.* **32**, 877–895 (2008).
- ¹⁸M. A. Kamoji, S. B. Kedare, and S. V. Prabhu, "Experimental investigations on single stage modified Savonius rotor," *Appl. Energy* **86**, 1064–1073 (2009).
- ¹⁹M. Amiri, A. R. Teymourtash, and M. Kahrom, "Experimental and numerical investigations on the aerodynamic performance of a pivoted Savonius wind turbine," *Proc. Inst. Mech. Eng. Part A: J. Power Energy* **231**(2), 87–101 (2016).
- ²⁰A. Chauvin and D. Benghrib, "Drag and lift coefficients evolution of a Savonius rotor," *Exp. Fluids* **8**(1-2), 118–120 (1989).
- ²¹M. N. I. Khan, M. T. Iqbal, M. Hinchey, and V. Mase, "Performance of Savonius rotor as a water current turbine," *J. Ocean Technol.* **4**(2), 71–83 (2009).
- ²²M. Nakajima, S. Iio, and T. Ikeda, "Performance of Savonius turbine for environmentally friendly hydraulic turbine," *J. Fluid Sci. Technol.* **3**(3), 410–419 (2008).
- ²³T. Sawada, M. Nahamura, and S. Kamada, "Blade force measurement and flow visualization of Savonius rotors," *Bull. JSME* **29**, 2095–2100 (1986).
- ²⁴N. K. Sarma, A. Biswas, and R. D. Misra, "Experimental and computational evaluation of Savonius hydrokinetic turbine for low velocity condition with comparison to Savonius wind turbine at the same input power," *Energy Convers. Manag.* **83**, 88–98 (2014).

- ²⁵V. Patel, G. Bhat, T. I. Eldho, and S. V. Prabhu, "Influence of overlap ratio and aspect ratio on the performance of Savonius hydrokinetic turbine," *Int. J. Energy Res.* **41**(6), 829–844 (2017).
- ²⁶S. Roy and U. K. Saha, "Review of experimental investigations into the design, performance and optimization of the Savonius rotor," *Proc. Inst. Mech. Eng. Part A: J. Power Energy* **227**(4), 528–542 (2013).
- ²⁷L. Chen, J. Chen, and Z. Zhang, "Review of the Savonius rotor's blade profile and its performance," *J. Renewable Sustainable Energy* **10**, 013306 (2018).
- ²⁸A. Kumar and R. P. Saini, "Performance parameters of Savonius type hydrokinetic turbine: A review," *Renewable Sustainable Energy Rev.* **64**, 289–310 (2016).
- ²⁹B. D. Plourde, J. P. Abraham, G. S. Mowry, and W. J. Minkowycz, "An experimental investigation of a large, vertical-axis wind turbine: Effects of venting and capping," *Wind Eng.* **35**, 213–220 (2011).
- ³⁰B. D. Altan, M. Atilgan, and A. Ozdamar, "An experimental study on improvement of a Savonius rotor performance with curtaining," *Exp. Therm. Fluid Sci.* **32**, 1673–1678 (2008).
- ³¹S. Roy and U. K. Saha, "An adapted blockage factor correlation approach in wind tunnel experiments of a Savonius-style wind turbine," *Energy Convers. Manag.* **86**, 418–427 (2014).
- ³²M. H. Mohamed, G. Janiga, E. Pap, and D. Thevenin, "Optimal blade shape of a modified Savonius turbine using an obstacle shielding the returning blade," *Energy Convers. Manag.* **52**, 236–242 (2011).
- ³³B. Zhang, B. Song, Z. Mao, and W. Tian, "A novel wake energy reuse method to optimize the layout for Savonius-type vertical axis wind turbines," *Energy* **121**, 341–355 (2017).
- ³⁴N. Alom and U. K. Saha, "Performance evaluation of vent-augmented elliptical-bladed Savonius rotors by numerical simulation and wind tunnel experiments," *Energy* **152**, 277–290 (2018).
- ³⁵M. Shiono, K. Suzuki, and S. Kiho, "Output characteristics of Darrieus water turbine with helical blades for tidal current generations," in *Proceedings of the Twelfth International Offshore and Polar Engineering Conference*, Kitakyushu, Japan (2002), pp. 859–864.
- ³⁶P. Marsh, D. Ramnuthugala, I. Penesis, and G. Thomas, "Numerical investigation of the influence of blade helicity on the performance characteristics of vertical axis tidal turbines," *Renewable Energy* **81**, 926–935 (2015).
- ³⁷P. K. Talukdar, A. Sardar, V. Kulkarni, and U. K. Saha, "Parametric analysis of model Savonius hydrokinetic turbines through experimental and computational investigations," *Energy Convers. Manag.* **158**, 36–49 (2018).
- ³⁸P. K. Talukdar, V. Kulkarni, D. Dehingia, and U. K. Saha, "Evaluation of a model helical bladed hydrokinetic turbine characteristics from in-situ experiments," in ASME 2017 11th International Conference on Energy Sustainability Paper No. ES2017-3490, Charlotte, NC, USA, June 26–30, 2017.
- ³⁹B. Altan and M. Atilgan, "An experimental and numerical study on the improvement of the performance of Savonius wind rotor," *Energy Convers. Manag.* **49**, 3425–3432 (2008).
- ⁴⁰B. Yang and C. Lawn, "Fluid dynamic performance of a vertical axis turbine for tidal currents," *Renewable Energy* **36**, 3355–3366 (2011).
- ⁴¹K. Kacprzak, G. Liskiewicz, and K. Sobczak, "Numerical investigation of conventional and modified Savonius wind turbines," *Renewable Energy* **60**, 578–585 (2013).
- ⁴²J. P. Abraham, B. D. Plourde, G. S. Mowry, E. M. Sparrow, and W. J. Minkowycz, "Numerical simulation of fluid flow around a vertical-axis turbine," *J. Renewable Sustainable Energy* **3**, 033109 (2011).
- ⁴³B. D. Plourde, J. P. Abraham, G. S. Mowry, and W. J. Minkowycz, "Simulations of three-dimensional vertical-axis turbines for communications applications," *Wind Eng.* **36**, 443–454 (2012).
- ⁴⁴A. Kumar and R. P. Saini, "Performance analysis of a Savonius hydrokinetic turbine having twisted blades," *Renewable Energy* **108**, 502–522 (2017).
- ⁴⁵A. Banerjee, S. Roy, P. Mukherjee, and U. K. Saha, "Unsteady flow analysis around an elliptic-bladed Savonius-style wind turbines," in ASME Gas Turbine India Conference, Paper No. GTINDIA 2014-8141, New Delhi, India, December 15–17, 2014.
- ⁴⁶S. Roy and A. Ducoin, "Unsteady analysis on the instantaneous forces and moment arms acting on a novel Savonius-style wind turbine," *Energy Convers. Manag.* **121**, 281–296 (2016).
- ⁴⁷M. Nasef, W. El-Askary, A. AbdEL-Hamid, and H. Gad, "Evaluation of Savonius rotor performance: Static and dynamic studies," *J. Wind Eng. Ind. Aerodyn.* **123**, 1–11 (2013).
- ⁴⁸S. Roy and U. K. Saha, "Review on the numerical investigations into the design and development of Savonius wind rotors," *Renewable Sustainable Energy Rev.* **24**, 73–83 (2013).
- ⁴⁹S. J. Kline and F. A. McClintock, "Describing uncertainties in single-sample experiments," *Mech. Eng.* **75**, 3–8 (1953).
- ⁵⁰R. J. Moffat, "Describing the uncertainties in experimental results," *Exp. Therm. Fluid Sci.* **1**(1), 3–17 (1988).
- ⁵¹N. Fujisawa and F. Gotoh, "Experimental study on the aerodynamic performance of a Savonius rotor," *J. Sol. Energy Eng.* **116**(3), 148–152 (1994).
- ⁵²A. Sanusi, S. Soepraman, S. Wahyudi, and L. Yuliati, "Experimental study of combined blade Savonius wind turbine," *Int. J. Renewable Energy Res.* **6**(2), 614–619 (2016).
- ⁵³P. N. Shankar, "Development of vertical axis wind turbines," *Proc. Indian Acad. Sci. C2*, 49–66 (1979).
- ⁵⁴K. V. Rabah and B. M. Osawa, "Design and field testing of Savonius wind pump in east Africa," in International Report, International Centre for Theoretical Physics, International Atomic Energy Agency and United Nations Educational Scientific and Cultural Organization, Trieste, Italy, 1995.
- ⁵⁵A. J. Alexander and B. P. Holownia, "Wind tunnel tests on a Savonius rotor," *J. Wind Eng. Ind. Aerodyn.* **3**(4), 343–351 (1978).
- ⁵⁶M. H. Ali, "Experimental comparison study for Savonius wind turbine of two and three blades at low wind speed," *Int. J. Mod. Eng. Res.* **3**(5), 2978–2986 (2013).
- ⁵⁷K. Golecha, T. I. Eldho, and S. V. Prabhu, "Performance study of modified Savonius water turbine with two deflector plates," *Int. J. Rotating Mach.* **2012**, 679247.
- ⁵⁸L. Chen, J. Chen, H. Xu, H. Yang, C. Ye, and D. Liu, "Wind tunnel investigation on the two- and three-blade Savonius rotor with central shaft at different gap ratio," *J. Renewable Sustainable Energy* **8**, 013303 (2016).
- ⁵⁹K. Irabu and J. N. Roy, "Study of direct force measurement and characteristics on blades of Savonius rotor at static state," *Exp. Therm. Fluid Sci.* **35**(4), 653–659 (2011).
- ⁶⁰P. Jaohindy, S. McTavish, F. Garde, and A. Bastide, "An analysis of the transient forces acting on Savonius rotors with different aspect ratios," *Renewable Energy* **55**, 286–295 (2013).